LETTER

doi:10.1038/nature10787

Quantum-coherent coupling of a mechanical oscillator to an optical cavity mode

E. Verhagen[1]*, S. Deléglise[1]*, S. Weis[1,2]*, A. Schliesser[1,2]* & T. J. Kippenberg[1,2]

Optical laser fields have been widely used to achieve quantum control over the motional and internal degrees of freedom of atoms and ions[1,2], molecules and atomic gases. A route to controlling the quantum states of macroscopic mechanical oscillators in a similar fashion is to exploit the parametric coupling between optical and mechanical degrees of freedom through radiation pressure in suitably engineered optical cavities[3–6]. If the optomechanical coupling is 'quantum coherent'—that is, if the coherent coupling rate exceeds both the optical and the mechanical decoherence rate—quantum states are transferred from the optical field to the mechanical oscillator and vice versa. This transfer allows control of the mechanical oscillator state using the wide range of available quantum optical techniques. So far, however, quantum-coherent coupling of micromechanical oscillators has only been achieved using microwave fields at millikelvin temperatures[7,8]. Optical experiments have not attained this regime owing to the large mechanical decoherence rates[9] and the difficulty of overcoming optical dissipation[10]. Here we achieve quantum-coherent coupling between optical photons and a micromechanical oscillator. Simultaneously, coupling to the cold photon bath cools the mechanical oscillator to an average occupancy of 1.7 ± 0.1 motional quanta. Excitation with weak classical light pulses reveals the exchange of energy between the optical light field and the micromechanical oscillator in the time domain at the level of less than one quantum on average. This optomechanical system establishes an efficient quantum interface between mechanical oscillators and optical photons, which can provide decoherence-free transport of quantum states through optical fibres. Our results offer a route towards the use of mechanical oscillators as quantum transducers or in microwave-to-optical quantum links[11–15].

Mechanical oscillators are at the heart of many precision experiments and can exhibit exceptionally low dissipation. The possibility of controlling the quantum states of engineered micro- or nano-mechanical oscillators has been a subject of long-standing interest[3,16]. Recent experiments have successfully prepared such devices in their quantum ground state, either using standard cryogenic techniques[7] or via dynamical back-action cooling[8,10]. Full control over the quantum state of a mechanical oscillator can be achieved by coupling it to an auxiliary system—whose quantum state can be controlled and measured—under the condition that the coherent coupling rate exceeds the decoherence rate of each of the subsystems. Such quantum-coherent coupling and control at the single-phonon level has been recently demonstrated in the microwave domain by achieving strong coupling of a gigahertz piezoelectrical dilatation oscillator to a (frequency-degenerate) superconducting qubit[7]. Moreover, an electromechanical system has reached the quantum-coherent regime using parametric coupling of a megahertz micromechanical oscillator to a gigahertz microwave resonator[8,17]. Achieving quantum-coherent coupling in the optical domain would provide an interface between mechanical quantum states and optical fields, whose low thermal occupancy at room temperature allows decoherence-free propagation of quantum states out of a cryogenic environment and which can be coupled to a variety of quantum systems. Additionally, optical techniques benefit from the wide availability of quantum-limited detection techniques. In fact, simultaneous achievement of quantum-coherent coupling in the optical and microwave domain provides the possibility of realizing optical-to-microwave conversion of quantum states[15].

Parametric optomechanical coupling occurs in an optical microcavity that simultaneously exhibits a mechanical resonator mode, whose displacement alters the optical resonance frequency. The coupling can be described by the interaction Hamiltonian $H=\hbar g_0\hat{a}^\dagger\hat{a}\left(\hat{b}^\dagger+\hat{b}\right)$, where $\hat{a}$ ($\hat{a}^\dagger$) and $\hat{b}$ ($\hat{b}^\dagger$) are the photon and phonon annihilation (creation) operators, respectively, $\hbar$ is the reduced Planck constant and g_0 is the vacuum optomechanical coupling rate. In the resolved sideband regime (where the mechanical resonance frequency Ω_m exceeds the cavity energy decay rate κ), with an intense laser tuned close to the lower optomechanical sideband, one obtains in the rotating wave approximation the effective Hamiltonian

$$H=\hbar g\left(\hat{a}\hat{b}^\dagger+\hat{a}^\dagger\hat{b}\right) \qquad (1)$$

for the operators $\hat{a}$ and $\hat{b}$ now displaced by their steady state values. We have introduced here the field-enhanced coupling rate[18–20] $g=\sqrt{\bar{n}_\mathrm{c}}g_0$, where $\bar{n}_\mathrm{c}$ denotes the average number of photons in the cavity. In the absence of decoherence, the unitary evolution given by equation (1) corresponds to swapping of the (displaced) optical and mechanical quantum states with a period of $2\pi/\Omega_\mathrm{c}$, where $\Omega_\mathrm{c}=2g$ is the coherent coupling rate, that is, the rate at which the two systems exchange energy. This state swapping is at the heart of most quantum control protocols[11–14,21,22]. In practice, however, this unitary evolution is compromised by the coupling of both degrees of freedom to their respective environments. Hence, it is important for Ω_c to exceed both the optical decoherence rate κ and the relevant mechanical decoherence rate γ. If the mechanical linewidth is limited by dissipation (as is the case in our system[23]), the mechanical decoherence is caused by energy relaxation to the hot environment. Thus, both decoherence rates are defined here as the inverse of the time needed for a single excitation to be lost into the environment. Importantly, the mechanical mode is coupled to an environment that generally has a large thermal occupancy $\bar{n}_\mathrm{m}\approx k_\mathrm{B}T/\hbar\Omega_\mathrm{m}$ (where k_B is Boltzmann's constant and T is temperature) owing to the relatively small mechanical frequency. Therefore, the mechanical decoherence rate $\gamma=\Gamma_\mathrm{m}(\bar{n}_\mathrm{m}+1)\approx k_\mathrm{B}T/\hbar Q_\mathrm{m}$ (where $Q_\mathrm{m}=\Omega_\mathrm{m}/\Gamma_\mathrm{m}$; refs 1, 14) is much larger than the dissipation rate Γ_m. This means that the strong coupling regime $\Omega_\mathrm{c}>(\kappa,\Gamma_\mathrm{m})$ (ref. 9) does not suffice to enable quantum control, in contrast to the situation in atomic cavity quantum electrodynamics[2] or in resonant coupling to superconducting qubits of sufficiently high frequency[7]. Instead, for parametrically coupled systems the more stringent condition $\Omega_\mathrm{c}>(\kappa,\gamma)$ signals the relevant regime, which we call quantum-coherent coupling.

Here we realize quantum-coherent coupling of an optical cavity field to a micromechanical oscillator. In this regime, the system is

[1]Ecole Polytechnique Fédérale de Lausanne (EPFL), 1015 Lausanne, Switzerland. [2]Max-Planck-Institut für Quantenoptik, Hans-Kopfermann-Strasse 1, 85748 Garching, Germany.
*These authors contributed equally to this work.

appropriately described as an optomechanical polariton whose decoherence time exceeds the period of the Rabi oscillations between light and mechanics. Although the ground state has recently been reported with optical cooling[10], in that work Ω_c was much smaller than κ. In contrast, the present system achieves a coupling rate exceeding both the optical and mechanical decoherence rates, thereby satisfying the necessary conditions for full control of the quantum state of a mechanical oscillator with optical fields[9,12–14,21,22]. The experimental setting is a micro-optomechanical system in the form of a spoke-anchored toroidal optical microcavity[24]. Such devices exhibit whispering gallery mode resonances of high quality factor (with a typical cavity decay rate $\kappa/2\pi < 10$ MHz) coupled to mechanical radial breathing modes via radiation pressure[25]. The vacuum optomechanical coupling rate $g_0 = (\omega_c/R)x_{ZPM}$ can be increased by reducing the radius R of the cavity (here ω_c is the optical cavity resonance frequency and x_{ZPM} is the zero point motion). However, the larger per photon force $\hbar\omega_c/R$ is then usually partially compensated by the increase in the mechanical resonance frequency Ω_m—and correspondingly smaller zero point motion, given by $x_{ZPM} = \sqrt{\hbar/(2m_{eff}\Omega_m)}$ (where m_{eff} is the effective oscillator mass). Moreover, small structures also generally feature larger dissipation through clamping losses. To compensate these opposing effects, we use an optimized spoke-anchor design (see Fig. 1 and Supplementary Information) that maintains low clamping losses and a moderate mechanical resonance frequency while reducing the dimensions of the structure. Devices fabricated in this manner (with $R = 15$ μm) exhibited coupling rates as high as $g_0 = 2\pi \times 3.4$ kHz for a resonance frequency of 78 MHz and a critically coupled sideband factor $\Omega_m/\kappa = 11$.

To reduce the mechanical decoherence rate $\gamma \approx \Gamma_m \bar{n}_m$, the microcavity is embedded in a ^{3}He cryostat (minimum temperature $T_{min} = 650$ mK)[26]. A continuous-wave Ti:sapphire laser beam, whose phase and amplitude quadrature noises are quantum-limited for the Fourier frequencies of interest, is coupled to the microcavity using a tapered optical fibre. The weak mechanical displacement fluctuations are recorded by measuring the phase fluctuations imprinted on the field emerging from the cryostat using balanced homodyne detection. Whereas the coherent coupling rate Ω_c can be determined unambiguously by probing the coherent response of the system[27], the mechanical decoherence rate is affected in a non-trivial way by the light-absorption-dependent sample temperature and the mechanical mode's coupling to its environment, which is dominated by two-level fluctuators at cryogenic temperatures[23,26]. In order to systematically assess the aforementioned effects on the decoherence rate, the coupling laser's frequency $\omega_l = \omega_c + \Delta$ (where Δ denotes the laser detuning) is varied in the vicinity of the lower mechanical sideband, while keeping the launched power constant. This allows the displaced cavity mode $\hat{a}$ (of frequency $|\Delta|$) to be brought in and out of resonance with the mechanical mode $\hat{b}$ (of frequency Ω_m). For each detuning point, we acquire the coherent response of the system to an optical excitation of swept frequency $\omega_l + \Omega_{mod}$ in a first step (Ω_{mod} is the frequency difference from the coupling laser). These spectra (Fig. 2a) allow us to determine all parameters of the model characterizing the optomechanical interaction (Supplementary Information). For large detunings $|\Delta| > \Omega_m$, they essentially feature a Lorentzian response of width κ and centre frequency $|\Delta|$. The sharp dip at $\Omega_{mod} \approx \Omega_m$ originates from optomechanically induced transparency[27] (OMIT), and for $\Omega_m = -\Delta$, its width is approximately Ω_c^2/κ. The coupling rate, as derived from a fit of the coherent response for a laser power of 0.56 mW, is $\Omega_c = 2\pi \times (3.7 \pm 0.05)$ MHz (corresponding to an intracavity photon number of $\bar{n}_c = 3 \times 10^5$).

Additionally, for each value of the detuning, the noise spectrum of the homodyne signal is recorded in the absence of any external excitation (Fig. 2b). The observed peak represents the phase fluctuations imprinted on the transmitted light by the mechanical mode's thermal motion. The constant noise background on these spectra is the shot-noise level for the (constant) laser power used throughout the laser sweep (see Supplementary Information for details). Importantly, the amplitude of the peak is determined by the coupling to and the temperature of the environment, and therefore allows us to extract the mechanical decoherence rate. All parameters now having been measured, it is moreover possible to retrieve the mechanical displacement spectrum (Fig. 2c inset). As can be seen, for detunings close to the sideband, when the (displaced) optical and mechanical modes are degenerate, the fluctuations are strongly reduced. This effect of optomechanical resolved sideband cooling[28] can be understood in a simple picture: in the regime $\Omega_c \ll \kappa$, the optical decay is faster than the swapping between the vacuum in the displaced optical field and the thermal state in the mechanical oscillator. In this case, the mechanical oscillator is coupled to an effective optical bath at near-zero thermal occupancy $\bar{n}_{min}$ with the rate $\Gamma_{cool} = \Omega_c^2/\kappa$. Ideally, $\bar{n}_{min} = \kappa^2/16\Omega_m^2 \ll 1$ is governed by non-resonant Stokes terms $\hat{a}^\dagger\hat{b}^\dagger + \hat{a}\hat{b}$ neglected in the Hamiltonian (equation (1))[18,19].

Evaluating the mechanical decoherence rate for $\Delta = -\Omega_m$ at a cryostat set point of 0.65 K, we find $\gamma = 2\pi \times (2.2 \pm 0.2)$ MHz—significantly smaller than Ω_c. Simultaneously, the average occupancy of the mechanical mode is reduced to $\bar{n} = 1.7 \pm 0.1$ (corresponding to $37 \pm 4\%$ ground state occupation), which is limited by the onset of normal mode splitting. Indeed, as Ω_c approaches κ, the thermal fluctuations are only partially dissipated into the optical bath, and are partially written back onto the mechanics after one Rabi cycle.

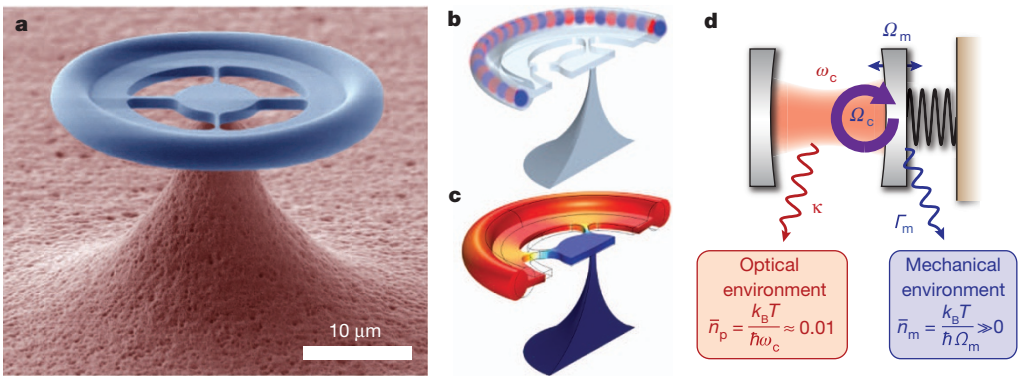

Figure 1 | Optomechanical microresonators. **a**, False-colour scanning electron micrograph of a spoke-anchored toroidal resonator 31 μm in diameter used for the optomechanical experiments reported in this work. **b**, Sketch of an optical whispering gallery mode in the microresonator (colours indicate optical phase). **c**, Simulated displacement (exaggerated for clarity) of the fundamental radial breathing mode of the structure. **d**, Equivalent optomechanical Fabry–Pérot cavity: quantum-coherent coupling is achieved when the enhanced coupling rate Ω_c is comparable to or exceeds the optical and mechanical decoherence rates ($\kappa, \Gamma_m\bar{n}_m$). Owing to the large asymmetry between mechanical and optical frequencies, the occupancies of the two environments are widely different.

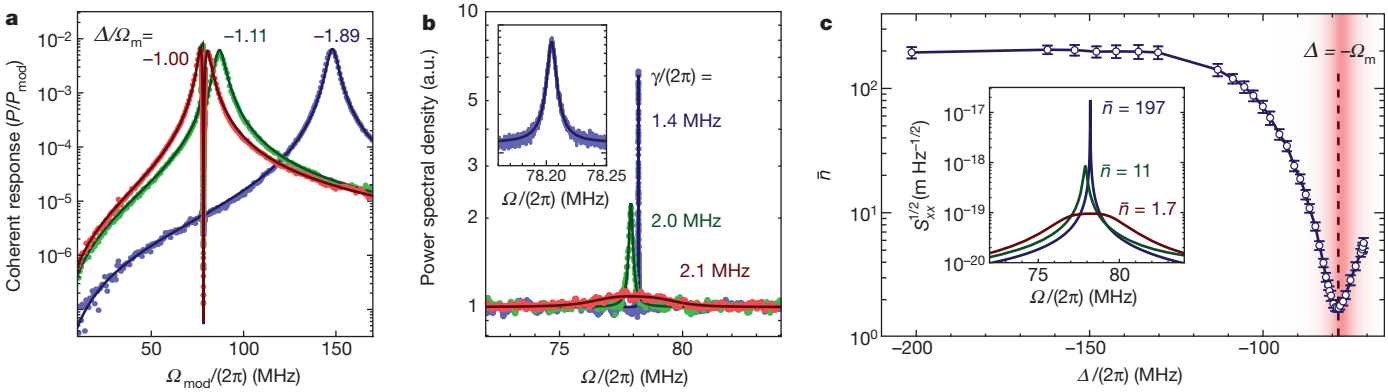

Figure 2 | Optomechanical interaction in the weak coupling regime ($\Omega_c \lesssim \kappa/2$). **a**, The coherent response of the system is obtained by sweeping a weak probe beam (at frequency $\omega_l + \Omega_{mod}$) over the cavity resonance and recording the homodyne signal P (normalized to the power P_{mod} used to create the probe beam). The fitted detuning (Δ/Ω_m) is indicated for each of the traces. The fit provides accurate estimation of the coupling rate Ω_c via the OMIT window (Supplementary Information). **b**, The measured Brownian noise spectrum in the absence of a coherent probe for each of the detunings in **a**. The spectra are corrected for the detector response and a small contribution of Guided Acoustic Wave Brillouin scattering (GAWBS) in the fibres (see Supplementary Information). The inset shows a close-up of the spectrum obtained for $\Delta/\Omega_m = -1.89$. The indicated decoherence rates γ are deduced from the amplitude of each noise spectrum (curves show the result of the model with fitted γ). **c**, Retrieved occupancy as a function of detuning. The minimum occupancy is 1.7 ± 0.1, meaning that the oscillator has a $37 \pm 4\%$ probability of occupying its ground state. The inset shows the inferred mechanical displacement spectral density S_{xx} for detunings used in **a** and **b** calculated using the extracted parameters. Error bars, estimated s.d. (see Supplementary Information).

We subsequently increase the strength of the coupling field to reach $\Omega_c \approx \kappa$. The signature of normal mode splitting[9,17,19,20] can be seen from both the coherent response and the fluctuation spectra (Fig. 3). Both detuning series exhibit a clear anti-crossing, the splitting frequency Ω_c being 5.7 MHz. Note that, in contrast to microwave experiments[8], no squashing is observed in the normal mode splitting data. The decoherence rate (Fig. 3d) is slightly raised compared to Fig. 2 owing to laser heating and a higher buffer gas temperature of 0.8 K, amounting to $\gamma = 2\pi \times (5.6 \pm 0.9)$ MHz at the lower mechanical sideband. We hence demonstrate $\Omega_c/\gamma = 1.0$, which constitutes an improvement of four orders of magnitude over the only previous work demonstrating strong coupling in the optical domain[9], and brings the system into the regime of quantum-coherent coupling. Even though all observed signatures are consistent with classical behaviour, entering this regime opens the door to preparation and control of non-classical states of mechanical motion with light.

As a proof of principle and as a first classical illustration of the potential of time-domain experiments, we demonstrate the dynamical exchange of a pulsed coherent excitation between the optical and mechanical degrees of freedom. By measuring the homodyne signal upon launching a weak pulse resonant with the cavity in the presence of the detuned coupling field (Fig. 4a), it is possible to directly observe the coherent exchange of energy. In the regime of weak coupling, the optical pulse excites the mechanical mode to a finite oscillation amplitude,

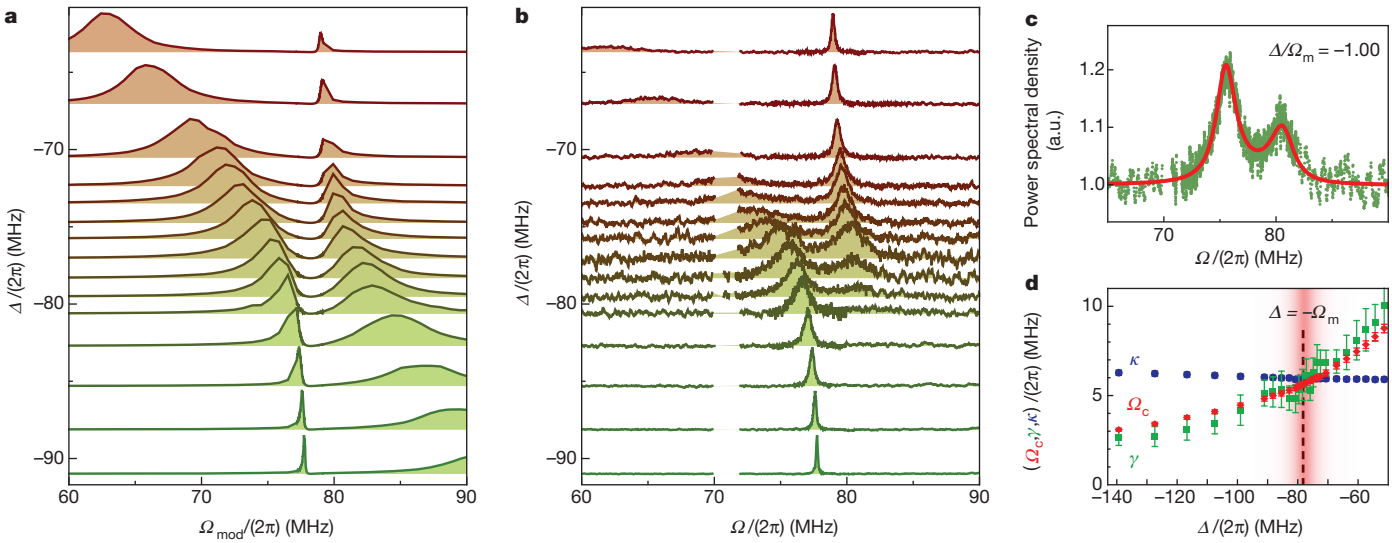

Figure 3 | Quantum-coherent coupling. **a**, **b**, The coherent optical response (**a**) and the incoherent mechanical noise spectrum (**b**) for various detunings of the coupling laser (with constant power $P = 1.4$ mW). All curves are normalized, and vertically displaced by the detuning. Evident in both panels is the avoided crossing which originates from optomechanical normal mode splitting. A second much more weakly coupled mechanical mode at 71 MHz is omitted and the curves are shaded for clarity. **c**, Homodyne noise spectrum obtained for $\Delta = -\Omega_m$. The red line is a fit of the model. Only the decoherence rate (determining the amplitude) is fitted, while the shape is fixed through the parameters determined from the coherent response. **d**, Comparison of the mechanical (green) and optical (blue) decoherence rates with the coherent coupling rate (red) as a function of detuning. The increase of γ close to resonance reflects heating of the cavity owing to the larger amount of absorbed light. On the lower mechanical sideband, where the interaction is resonant, the decoherence rates are comparable to the coupling rate, achieving quantum-coherent coupling. Error bars, estimated s.d. (see Supplementary Information).

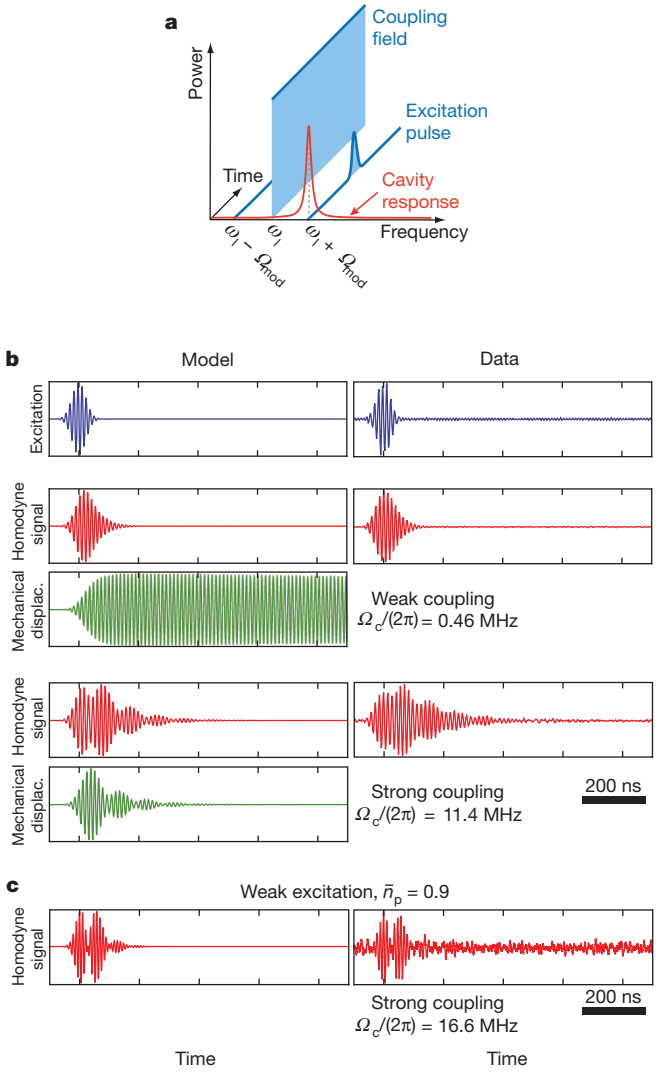

Figure 4 | Coherent exchange between the optical field and the micromechanical oscillator. This exchange is probed in the time domain as measured ('Data') and as calculated numerically ('Model'). A modulation pulse (blue traces) applied to the phase modulator creates an excitation pulse probing the dynamics of the optomechanical system in the presence of the coupling field. The response of the system is encoded into the homodyne output signal (red traces). Using the full model of the system, the mechanical displacement can be simulated in addition (green traces). **a**, Schematic of the excitation scheme, with the cavity frequency response sketched as the red curve. **b**, In the regime of weak coupling (upper panels), the optical output pulse exhibits only a weak signature of the mechanical ringdown excited by the short burst of radiation pressure. In the case of strong coupling (lower panels) the modulated envelopes of the time-domain response indicate several cycles of oscillation between coherent optical and mechanical excitations of the system. **c**, Results for weak excitation (average photon number $\bar{n}_p = 0.9$) and strong coupling.

which decays slowly at the optically damped mechanical dissipation rate. This in turn only imprints a weak signature on the homodyne signal (Fig. 4b). Increasing the laser power, we reach $\Omega_c/2\pi = 11.4\,\mathrm{MHz} > \kappa/2\pi = 7.1\,\mathrm{MHz}$, and the envelope of the homodyne signal—corresponding to the amplitude of the measured sideband field—undergoes several cycles of energy exchange with the mechanical oscillator, before it decays with a modified rate of $(\kappa + \Gamma_m)/2 \approx \kappa/2$, corresponding to the decay rate of the excited optomechanical polariton. Using our model (which has been matched to separately taken coherent response measurements), we can derive not only the homodyne signature—which reproduces our data very well—but also the expected mechanical oscillations resulting from this pulsed excitation. These reveal how the excitation cycles continuously between the optical and mechanical modes. Reducing the excitation further, so that one pulse contains less than one photon on average, a clear signature of several swapping cycles can still be observed (Fig. 4c). Although the average evolution observed here follows classical dynamics and is not affected by decoherence, replacing the weak coherent state in this experiment by a single photon[13,22] is expected to result in Rabi-like oscillation of the Fock state from optics to mechanics as the system resides in the quantum-coherent regime (which we have proved above on the basis of measurements of classical signatures). A repeated quadrature measurement yielding a bimodal distribution would then provide an unambiguous signature of the quantum nature of the state after the full swap[29].

Obtaining quantum-coherent coupling $\Omega_c \gtrsim (\gamma,\kappa)$ has several interesting consequences. It allows the mapping of elemental quantum states of the optical field onto the mechanical mode via the use of a time-dependent coupling field. For example, preparation of the mode in the ground state or the Fock state $|1\rangle$ can be efficiently achieved in this regime using a π-pulse which swaps the thermal state of the oscillator and the quantum state of the displaced optical field. Note that the manipulation of large quantum states becomes increasingly challenging because the lifetime of the number state $|n\rangle$ scales with $1/n$. In this context, it will be beneficial to reduce spurious laser heating and employ materials with low intrinsic loss, as well as to increase the optomechanical coupling rate by further miniaturization. The regime of quantum-coherent coupling demonstrated here has been proposed as a general quantum link between electromagnetic fields of vastly different frequencies—for example, different wavelengths in the optical spectrum or microwave and optical photons[12,15]. Electrical actuation of whispering gallery mode resonators has recently been demonstrated at an elementary level[30]. In this context, the efficient coupling of the demonstrated system to a low-loss single mode optical fibre is beneficial. Moreover, quantum-coherent coupling enables the use of the mechanical oscillator as a transducer to link otherwise incompatible elements in hybrid quantum systems, such as solid-state spin, charge, or superconducting qubits and propagating optical fields[14].

The reported experiments—which achieve quantum-coherent coupling between a micromechanical oscillator and an optical mode—represent an important step into the experimental investigation and optical quantum control of the most tangible harmonic oscillator: a mechanical vibration.

METHODS SUMMARY

The quoted value of g_0 is determined independently at room temperature via a calibrated phase modulation technique. The microcavity is evanescently coupled to a tapered optical fibre in a ^{3}He cryostat using piezoelectric positioning stages. For low optical power, the ^{3}He buffer gas enables thermalization of the resonator over the entire cryogenic temperature range in spite of its weak thermal anchoring to the substrate. A balanced homodyne detection scheme is employed, and a continuous wave Ti:sapphire laser is used to derive both the coupling field and the homodyne local oscillator. Care is taken to avoid excess noise in the coupling beam, as this would cause an effective increase of $\bar{n}_{min}$ and preclude any quantum state manipulation. In practice it has proven crucial to eliminate phase noise originating from guided acoustic wave Brillouin scattering in the optical fibres by engineering their acoustic modes using HF etching (Supplementary Information). For the time-domain experiments, the coupling laser's phase is modulated at the mechanical resonance frequency, with a Gaussian envelope of 54 ns duration, creating a pair of sidebands—one of which is resonant with the optical cavity—that contain on average ten quanta per pulse (Supplementary Information). Although the detection used is far from optimized for time-domain experiments, a signal-to-noise ratio of 40 is achieved in Fig. 4b by averaging 250,000 traces within two minutes.

Received 5 September; accepted 9 December 2011.

1. Wineland, D. J. *et al.* Experimental issues in coherent quantum-state manipulation of trapped atomic ions. *J. Res. Natl Inst. Stand. Technol.* **103,** 259–328 (1998).
2. Kimble, H. J. Strong interactions of single atoms and photons in cavity QED. *Phys. Scripta* **T76,** 127–137 (1998).

3. Braginsky, V. B. *Measurement of Weak Forces in Physics Experiments* (Univ. Chicago Press, 1977).
4. Kippenberg, T. J. & Vahala, K. J. Cavity optomechanics: back-action at the mesoscale. *Science* **321,** 1172–1176 (2008).
5. Favero, I. & Karrai, K. Optomechanics of deformable optical cavities. *Nature Photon.* **3,** 201–205 (2009).
6. Clerk, A. A., Devoret, M. H., Girvin, S. M., Marquardt, F. & Schoelkopf, R. J. Introduction to quantum noise, measurement, and amplification. *Rev. Mod. Phys.* **82,** 1155–1208 (2010).
7. O'Connell, A. D. *et al.* Quantum ground state and single-phonon control of a mechanical resonator. *Nature* **464,** 697–703 (2010).
8. Teufel, J. D. *et al.* Sideband cooling of micromechanical motion to the quantum ground state. *Nature* **475,** 359–363 (2011).
9. Gröblacher, S., Hammerer, K., Vanner, M. R. & Aspelmeyer, M. Observation of strong coupling between a micromechanical resonator and an optical cavity field. *Nature* **460,** 724–727 (2009).
10. Chan, J. *et al.* Laser cooling of a nanomechanical oscillator into its quantum ground state. *Nature* **478,** 89–92 (2011).
11. Zhang, J., Peng, K. & Braunstein, S. L. Quantum-state transfer from light to macroscopic oscillators. *Phys. Rev. A* **68,** 013808 (2003).
12. Tian, L. & Wang, H. Optical wavelength conversion of quantum states with optomechanics. *Phys. Rev. A* **82,** 053806 (2010).
13. Akram, U., Kiesel, N., Aspelmeyer, M. & Milburn, G. J. Single-photon opto-mechanics in the strong coupling regime. *N. J. Phys.* **12,** 083030 (2010).
14. Stannigel, K., Rabl, P., Sorensen, A. S., Zoller, P. & Lukin, M. D. Optomechanical transducers for long-distance quantum communication. *Phys. Rev. Lett.* **105,** 220501 (2010).
15. Regal, C. A. & Lehnert, K. W. From cavity electromechanics to cavity optomechanics. *J. Phys. Conf. Ser.* **264,** 012025 (2011).
16. Schwab, K. C. & Roukes, M. L. Putting mechanics into quantum mechanics. *Phys. Today* **58,** 36–42 (2005).
17. Teufel, J. D. *et al.* Circuit cavity electromechanics in the strong coupling regime. *Nature* **471,** 204–208 (2011).
18. Wilson-Rae, I., Nooshi, N., Zwerger, W. & Kippenberg, T. J. Theory of ground state cooling of a mechanical oscillator using dynamical backaction. *Phys. Rev. Lett.* **99,** 093901 (2007).
19. Marquardt, F., Chen, J. P., Clerk, A. A. & Girvin, S. M. Quantum theory of cavity-assisted sideband cooling of mechanical motion. *Phys. Rev. Lett.* **99,** 093902 (2007).
20. Dobrindt, J. M., Wilson-Rae, I. & Kippenberg, T. J. Parametric normal-mode splitting in cavity optomechanics. *Phys. Rev. Lett.* **101,** 263602 (2008).
21. Khalili, F. *et al.* Preparing a mechanical oscillator in non-Gaussian quantum states. *Phys. Rev. Lett.* **105,** 070403 (2010).
22. Romero-Isart, O. *et al.* Optically levitating dielectrics in the quantum regime: theory and protocols. *Phys. Rev. A* **83,** 013803 (2011).
23. Arcizet, O., Rivière, R., Schliesser, A., Anetsberger, G. & Kippenberg, T. J. Cryogenic properties of optomechanical silica microcavities. *Phys. Rev. A* **80,** 021803(R) (2009).
24. Anetsberger, G., Rivière, R., Schliesser, A., Arcizet, O. & Kippenberg, T. J. Ultralow-dissipation optomechanical resonators on a chip. *Nature Photon.* **2,** 627–633 (2008).
25. Kippenberg, T. J., Rokhsari, H., Carmon, T., Scherer, A. & Vahala, K. J. Analysis of radiation-pressure induced mechanical oscillation of an optical microcavity. *Phys. Rev. Lett.* **95,** 033901 (2005).
26. Rivière, R. *et al.* Optomechanical sideband cooling of a micromechanical oscillator close to the quantum ground state. *Phys. Rev. A* **83,** 063835 (2011).
27. Weis, S. *et al.* Optomechanically induced transparency. *Science* **330,** 1520–1523 (2010).
28. Schliesser, A., Rivière, R., Anetsberger, G., Arcizet, O. & Kippenberg, T. Resolved-sideband cooling of a micromechanical oscillator. *Nature Phys.* **4,** 415–419 (2008).
29. Lvovsky, A. I. *et al.* Quantum state reconstruction of the single-photon Fock state. *Phys. Rev. Lett.* **87,** 050402 (2001).
30. Lee, K. H., McRae, T. G., Harris, G. I., Knittel, J. & Bowen, W. P. Cooling and control of a cavity optoelectromechanical system. *Phys. Rev. Lett.* **104,** 123604 (2010).

Supplementary Information is linked to the online version of the paper at www.nature.com/nature.

Acknowledgements We acknowledge R. Rivière for early contributions to this project and E. Gavartin and I. Vázquez García for assistance in the early microfabrication phase. This work was supported by an ERC Starting Grant (SiMP), the DARPA/MTO ORCHID program through a grant from the AFOSR, the NCCR Quantum Science and Technology and the Swiss National Science Foundation. E.V. acknowledges a Rubicon Grant from the Netherlands Organization for Scientific Research (NWO), co-financed by a Marie Curie Cofund Action. S.D. is supported by a Marie Curie Individual Fellowship.

Author Contributions The cryogenic cooling, measurement, and sample design and fabrication was carried out jointly by S.D., E.V and S.W. The theoretical model for data analysis was developed by A.S. All authors discussed the experimental data and jointly wrote the manuscript. T.J.K. supervised the work.

Author Information Reprints and permissions information is available at www.nature.com/reprints. The authors declare no competing financial interests. Readers are welcome to comment on the online version of this article at www.nature.com/nature. Correspondence and requests for materials should be addressed to T.J.K. (tobias.kippenberg@epfl.ch).